Spatial Distribution of Trends and Seasonality in the Hemispheric Sea Ice Covers: 1978 - 1996

P. Gloersen, C. L. Parkinson, D. J. Cavalieri, J. C. Comiso, and H. J. Zwally

Oceans and Ice Branch, Laboratory for Hydrospheric Processes

NASA Goddard Space Flight Center

Greenbelt, Maryland 20771

Submitted to JGR Oceans 5.29.98

Spatial Distribution of Trends and Seasonality in the Hemispheric Sea Ice Covers: 1978 - 1996

P. Gloersen, C. L. Parkinson, D. J. Cavalieri, J. C. Comiso, and H. J. Zwally

Oceans and Ice Branch, Laboratory for Hydrospheric Processes

NASA Goddard Space Flight Center

Greenbelt, Maryland 20771

Summary:

We extend earlier analyses of a 9-year sea ice data set that described the local seasonal and trend variations in each of the hemispheric sea ice covers to the recently merged 18.2-year sea ice record from four satellite instruments. The seasonal cycle characteristics remain essentially the same as for the shorter time series, but the local trends are markedly different, in some cases reversing sign. The sign reversal reflects the lack of a consistent long-term trend and could be the result of localized long-term oscillations in the hemispheric sea ice covers. By combining the separate hemispheric sea ice records into a global one, we have shown that there are statistically significant net decreases in the sea ice coverage on a global scale. The change in the global sea ice extent, is $-0.01 \pm 0.003 \times 10^6$ km^2 per decade. The decrease in the areal coverage of the sea ice is only slightly smaller, so that the difference in the two, the open water within the packs, has no statistically significant change.

Abstract

We extend earlier analyses of a 9-year sea ice data set that described the local seasonal and trend variations in each of the hemispheric sea ice covers to the recently merged 18.2-year sea ice record from four satellite instruments. The seasonal cycle characteristics remain essentially the same as for the shorter time series, but the local trends are markedly different, in some cases reversing sign. The sign reversal reflects the lack of a consistent long-term trend and could be the result of localized long-term oscillations in the hemispheric sea ice covers. By combining the separate hemispheric sea ice records into a global one, we have shown that there are statistically significant net decreases in the sea ice coverage on a global scale. The change in the global sea ice extent, is $-0.01 \pm 0.003 \times 10^6$ km^2 per decade. The decrease in the areal coverage of the sea ice is only slightly smaller, so that the difference in the two, the open water within the packs, has no statistically significant change.

Introduction

We analyze the 18.2-year polar sea ice record produced from the data of the Scanning Multichannel Microwave Radiometer (SMMR) on board the NASA Nimbus 7 satellite [*Gloersen et al.*, 1992] and the Special Sensor Microwave/Imagers (SSMIs) on board three of the Defense Meteorological Satellite Program (DMSP) satellites, F8, 11, & 13. We extend, with revised methodology, the analysis done earlier on the 8.8-year sea ice data set produced from observations with the SMMR alone [*Gloersen and Campbell*, 1991; *Gloersen et al.*, 1996; and *Gloersen and Mernicky*, 1998]. The procedure for preparing the combined satellite data set from the four passive-microwave sensors is discussed in detail elsewhere [*Cavalieri et al.*, 1997 and this issue].

We examine first the global records of sea ice area and extent, obtained by combining the Arctic and Antarctic records, to determine their trend, seasonal oscillation, and interannual variability. Analysis of this combination is expected to provide additional insight into the global circulation system, e.g., the oscillations in the combined ice covers are reflected in various climate variables, such as absorption of solar radiation. Next, we examine the trends and seasonal oscillations in each element of the Arctic and Antarctic grids and show that the local decadal trends in some places are much larger and in others much smaller than their hemispheric or global averages. They are comparable to the amplitude of the local seasonal oscillations. We compare the results obtained here with the earlier results based on SMMR data alone, and discuss some important differences.

Methodology

We use both multiple ordinary least squares regression (MOLSR) and Band-Limited Regression (BLR) [*Gloersen and Campbell*, 1991] to analyze the SMMR/SSMI data set. The MOLSR invokes 12 linear components to produce a model fit of the gridded data at each grid point. These are described by the equation:

$$y = a_0 + a_1 t + \sum_{k=1}^{5} [a_{(2k-1)} \cos(2\pi kt/\tau) + a_{2k} \sin(2\pi kt/\tau)]$$

where τ is the annual cycle.

The BLR technique has been described in detail elsewhere [*Lindberg*, 1986; *Lindberg and Park*, 1987; *Kuo et al.*, 1990]. Briefly, the technique involves the application of a narrow-bandpass filter comprised of multiple prolate spheroid windows while determining the trend of the data series and its standard deviation. The F8 SSMI record contains a 42-day data gap deemed too large for the BLR technique to handle successfully. Therefore, the data gap was filled with values generated by a MOLSR model as described above, and the MOLSR coefficients were derived from part of the F8 SSMI data set consisting of 60 days before and 60 days after the gap.

The global sea ice record

The global records of sea ice area and extent are obtained by adding the separate Arctic [Parkinson et al., this issue] and Antarctic [*Zwally et al.*, in preparation] records of single-day observations, and are shown in Figure 1. As previously noted for the shorter SMMR record [*Gloersen and Campbell*, 1988; *Gloersen et al.*, 1992], the annual cycles in these records are double-peaked because of the near coincidence of the Antarctic maxima and the Arctic minima and because the Arctic troughs are narrower than the Antarctic peaks. The variability in the pattern reflects the interannual variability in the timing of the Antarctic maxima and the Arctic minima, presumably arising from the interannual variation in the atmospheric circulation patterns. The variation in the shape of the less distinct double minima is explained with a symmetrical argument.

The annual variation of the global sea ice area is approximately 39% of the mean, on average, and represents an annual change of about 10^{21} J in the amount of latent heat stored in the global sea ice cover, assuming an average seasonal sea ice zone cover thickness of 0.5 m [*Gloersen et al.*, 1992]. When spread over the course of a year and over about 10^{13} m^2 of seasonal sea ice zone area, the annual variation becomes about 30 Wm^{-2}, an order of magnitude smaller than the annual variation of insolation, but not negligible. A more significant effect is the corresponding change in surface albedo, which results in an order of magnitude annual change in the absorbed solar radiation at the ocean surface in the seasonal sea ice zone. Still more important is the two to three order of magnitude change in the rate of sensible heat exchange between the surface and the atmosphere

when the ocean surface becomes covered with ice [*Badgley*, 1966; *Maykut*, 1978]. This can play a significant role in atmospheric circulation [*Budd*, 1975; *Simmons and Budd*, 1990].

The difference of the two curves in Figures 1a and b results in a curve (Figure 1c) of open water within the packs. The mean value of the open water is 4.45×10^6 km^2. On average, the extrema are about 5.8×10^6 km^2 and 2.7×10^6 km^2, with about 5×10^5 km^2 of interannual variability in each extremum. There is no statistically significant trend in the global open water time series.

While separate analyses show a statistically significant sea ice extent decrease in the Arctic and increase in the Antarctic during this time period [*Cavalieri* et al., 1997; *Parkinson et al.*, this issue; *Zwally et al.*, in preparation], BRL analysis of the global sum of the two shows a statistically significant net decrease of $-0.01 \pm 0.003 \times 1\ 0^6$ km^2 per decade. The global ice area decreases by almost the same amount, $-0.009 \pm 0.002 \times 1\ 0^6$ km^2 per decade. The results are depicted in Figure 2. Also shown for comparison in Figure 2 are the extent, area, and open water within the pack data of Figure 1 subsequently smoothed with a Butterworth filter [*Parks and Burrus*, 1987] having a window width of 1 year. Neglecting the initial ½-year startup transient in the filtering process, the interannual undulations about the trend lines are about 5% of the mean values. The periodicities are a combination of the approximately 5-year oscillations in the north and 3-year oscillations in the south [*Cavalieri et al.*, 1997].

Areal distribution of the major hemispheric sea ice signals

The MOLSR was used at each grid point of the time series of hemispheric sea ice data maps to produce 12 maps, corresponding to the intercept, the slope, and the cosine/sine coefficients for five harmonics of the annual cycle. From these, we constructed 18.2-year means by adding the slope times the time interval of 9.1 years to the intercept, i.e. we selected the mid-point of the MOLSR trend line. The results are shown in Plates 1a and 1b.

In the central Arctic (Plate 1a.), the mean sea ice concentration for the 18.2-year interval discussed here is slightly lower than the 8.8-year mean described earlier for the SMMR-only data, using the same technique [*Gloersen et al.*, 1996]. The highest mean ice concentrations in the SMMR epoch are in the 96-100% range, while the largest means shown here are in the 92-96% range, and cover a smaller area than the earlier ones. For grid elements closer to the perimeter of the central Arctic pack, this disparity generally becomes greater, except for the Beaufort Sea, where it becomes less than in the SMMR-only analysis. The disparity is particularly striking in the Laptev Sea where, for instance, the mean open water is substantially closer to Novaya Zemlya in the longer period. Also, in the Greenland Sea, the mean ice concentrations are about 10% lower, and the "Odden" feature is smaller in extent for the longer period than for the shorter earlier period. Baffin Bay, on the other hand, is about the same for the two periods. These features are consistent with an overall decreasing Arctic ice cover.

In contrast, the Antarctic mean ice concentrations for the SMMR [*Gloersen and Mernicky*, 1998] and 18.2-year (Plate 1b.) periods are substantially the same, differing only in minor details of the isotach patterns. This is not necessarily inconsistent with an earlier finding that the Antarctic sea ice extent has a statistically significant increase in the 18.2-year period [*Cavalieri et al.*, 1997], since the small increase could easily fit within the 4% ice concentration steps shown in Plate 1b.

The next largest component in the hemispheric ice cover signal is what we call the seasonal cycle, i.e., the Fourier series of the first five harmonics of the annual cycle. Examination of the 18.2-year records of ice extent [*Cavalieri et al.*, 1997] reveal that, as expected, they are not monochromatic sinusoids. We approximate the amplitude of this signal by taking the rms of the amplitudes of the 10 Fourier components from our MOLSR fit. One needs to avoid over-interpretation of these results, as ringing of the fit in regions that are ice-free during parts of the cycle can cause the amplitudes in those regions to be slightly greater than half their mean values, which is not physically realizable.

The amplitudes of the seasonal cycle in the central Arctic are generally smaller for the 18.2-year period (Plate 1c.) than those for the SMMR period alone [*Gloersen et al.*, 1996]. For instance, the 0-4% amplitudes have expanded from the small area just north of the Canadian Archipelago observed with SMMR to cover much of the central Arctic in the longer time series. There is little disparity in the seasonal amplitudes in the Beaufort Sea near the coast, but in other perimeter areas the disparity actually increases. Of course, these general decreases in the local seasonal amplitudes are consistent with the general decreases in the local means.

As for the local means in the Antarctic, the local amplitudes of the seasonal cycles there are substantially the same for the 18.2-year (Plate 1d.) and the SMMR [*Gloersen & Mernicky*, 1998] periods. Again, this is consistent with a general lack of change in the local means.

Spatial distribution of the decadal trends in the hemispheric sea ice records

Trends obtained with the MOLSR procedure are included in the companion papers [*Parkinson et al.*, this issue; *Zwally et al.*, in preparation]. Here, we show the hemispheric local trends and their confidence levels as obtained by applying the BLR method to the time series of each grid point (Plate 2.). The results from each method are nearly the same, but the confidence levels obtained for the MOLSR (not shown) are orders of magnitude lower than those for the BLR approach. The range of local 9-year trends in the Arctic sea ice concentrations, -40% to +20%, observed previously for the SMMR data [*Gloersen et al.*, 1996] is much wider than the decadal trends observed for the 18.2-year period, <-17% to + 6% (Plate 2a.). This is probably a consequence of the presence of cyclic variations in the annual-to-decadal range even longer than the quasibiennial and quasiquadrennial oscillations observed earlier in the SMMR data [*Gloersen et al.*, 1996]. This possibility is underscored by the reversal of trend in some areas, e.g., in the Chukchi Sea. The most substantial decreases in sea ice in the 18.2-year period occur in the seas around Novaya Zemlya, the Sea of Okhotsk, and the Chukchi and Greenland seas. These decreases are largely counterbalanced by increases in Baffin Bay, the Gulf of St. Lawrence, the Bering and Labrador Seas, and in the Arctic

Ocean just north of Greenland and Ellesmere Island. Thus again in this longer period, the small overall decrease in Arctic sea ice area [*Parkinson et al.*, this issue] is comprised of much larger local increases and decreases, as seen also in the regional results [*ibid*].

In the Antarctic, the reversal of trend from the SMMR data [*Gloersen and Mernicky*, 1998] to the 18.2-year data set is more widespread, being the rule rather than the exception. As in the Arctic, the range of decadal trends in the Antarctic has been reduced, in this case from -40% to +32% for the SMMR data to -15% to +11% for the 18.2-year data (Plate 2b.). The rate of decadal decrease in the approximate location of the Weddell Polynya [*Zwally et al.*, 1985] has changed from -24 to -28% for the SMMR data to about -5% here (and hence, an earlier prediction of the imminent reappearance of the Weddell Polynya [*Gloersen and Mernicky*, 1998] is refuted), and the region has moved to the west. As anticipated [*Parkinson*, 1994], some regions subsequently reveal trend reversal. The strongest trend reversal is in the Ross Sea. During the SMMR years, the ice concentration in the eastern portion of the Ross Sea was increasing at a maximum rate of 28-32% per decade, while in the western portion it was decreasing at a maximum rate of 40%. In contrast, during the 18.2-year period, the eastern portion decreased at a maximum rate of about 5% per decade while the western portion increased at a maximum rate of about 11%. Comparing the shorter (SMMR) and longer (18.2-year) records of the Weddell Sea reveals more complicated behavior, containing both monotonic rate decreases, e.g., in the vicinity of the former Weddell Polynya, as well as trend reversals, e.g., near the Larsen Ice Shelf: -8-12% changing to about +2%. North of the Filchner Ice Shelf, there was an increase in the positive decadal trend of about 10%. These relatively large local trends average out to a small, but statistically significant, overall increase in the ice concentrations, as

indicated by the ice area [*Cavalieri et al.*, 1997; *Zwally et al.*, in preparation]. As in the Arctic, these signal changes are indicative of the presence of long-period oscillations.

A closer look at the seasonal cycles in the hemispheric sea ice signals

As indicated earlier, the MOLSR procedure produces coefficients for the first five harmonics of the annual cycle, yielding both amplitude and phase information. The spatial distribution of the amplitudes and phases of the fundamental (annual cycle) in the Arctic and Antarctic are shown in Plate 3. The local amplitudes of both are generally smaller than those of the seasonal cycles (Plates 1c and 1d).

The local phases of the annual cycle in the Antarctic sea ice concentrations are very similar for the shorter and longer time series, indicating long-term stability in this component of the variability. One, at first look, apparently large difference in the shorter [*Gloersen and Mernicky*, 1998, Plate 1d] and the present, longer (Plate 3b) time series can be seen off the Filchner Ice Shelf. However, since the phase scale wraps around from $+\pi$ to $-\pi$, the phase difference is actually quite small. Qualitatively, the phase patterns follow the sequential growth and decay of the ice pack as depicted in the 9-year averages by month presented elsewhere [*Gloersen et al.*, 1992]. However, there are some differences in detail in the two sets of patterns which are not yet understood.

The Arctic displays much smaller variation in the local phases compared to the Antarctic, again following the annual growth and decay of the ice pack as depicted in the nine-year averages by month [*Gloersen et al.*, 1992]. The phases near the coastlines of Norway, England, and Iceland are spurious, and probably reflect imperfections in the coastline cleanup algorithm that were applied to these data [*Cavalieri et al.*, 1997 and this issue].

The amplitudes of the second (semi-annual) and third harmonics of the Arctic and Antarctic sea ice concentrations are shown in Plate 4. In the Arctic, the semi-annual oscillation is as high as ±25% (Baffin Bay and the Laptev, Kara, and eastern Chukchi Seas). In the central Arctic, it is even greater than the annual cycle. The semiannual cycle is generally largest in the perimeter seas.

In the Antarctic, there is widespread comparability between the amplitudes of the annual and semiannual cycles. Except for the region of the Indian Ocean, the semiannual cycle is largest in the interior of the ice pack, unlike the Arctic.

The amplitudes of the third harmonic in both hemispheres (Plate 4c and 4d.) are generally less than ±15%. The fourth and fifth harmonics (not shown) are even smaller.

Summary

By combining the separate hemispheric sea ice records into a global one, we have shown that there are statistically significant net decreases in the sea ice coverage on a global scale. The change in the

global sea ice extent, is $-0.01 \pm 0.003 \times 10^6$ km^2 per decade. The decrease in the areal coverage of the sea ice is only slightly smaller, so that the difference in the two, the open water within the packs, has no statistically significant change. The net seasonal variation in the global pack is about 39% of the global mean, and when integrated over a year the latent heat needed to melt this amount of ice represents about 10% of the annual variation in the global insolation.

In comparing the 18-year local means of the hemispheric ice cover concentrations with the earlier 9-year records, we find that the 18-year means in the central Arctic are smaller than the 9-year ones, in keeping with the long-term negative trends in those localized areas. The trends noted in the Antarctic, however are too small to be observed as increases in the local means when comparing the two records. Examination of the local trends in the two records reveals smaller trends, or even reversal of the directions of the trends, in the longer one. We interpret these observations as an indication of long-term oscillations in the hemispheric ice packs.

A modeled seasonal cycle has been produced for each of the polar map grid elements for each hemisphere. The coefficients for the model were obtained by multiple ordinary least squares fitting of the data. Comparison of the modeled seasonal cycles in the earlier 9- and present 18-year time spans of each hemisphere shows them to be largely the same, indicating stability in both the amplitude and phase of their monochromatic components.

References

Badgley, F.I., Heat budget at the surface of the Arctic Ocean, in *Proc. of the Symp. on the Arctic Heat Budget and Atmospheric Circulation,* J. O. Fletcher, ed., pp. 267-277, 1966.

Budd, W. F., Antarctic sea ice variations from satellite sensing in relation to climate, *J. Glaciol.* **15**, 417-426, 1975.

Cavalieri, D. J., P. Gloersen, C. L. Parkinson, J. C. Comiso, and H. J Zwally, Observed asymmetry in global sea ice changes, *Science* **278**, 1104-1106, 1997.

Cavalieri, D. J., C. L. Parkinson, P. Gloersen, J. C. Comiso, and H. J Zwally, Deriving long-term time series from satellite passive-microwave multisensor data sets, *this issue*.

Gloersen, P. and W.J. Campbell, Variations in the Arctic, Antarctic, and global sea ice covers during 1978-1987 as observed with the Nimbus-7 Scanning Multichannel Microwave Radiometer, *J. Geophys. Res.* **93**, 10,666-10,674, 1988.

Gloersen, P., and W. J. Campbell, Recent variations in Arctic and Antarctic sea ice covers, *Nature* **352**, 33-36, 1991.

Gloersen, P., W. J. Campbell, D. J. Cavalieri, J. C. Comiso, C. L. Parkinson, and H. J. Zwally, Arctic and Antarctic sea ice, 1978-1987: Satellite passive-microwave observations and analysis, *NASA SP-511*, Washington D.C., 1992.

Gloersen, P., J. Yu, and E. Mollo-Christensen, Oscillatory behavior in Arctic sea ice concentrations, *J. Geophys. Res,* **101**, 6641-6650, 1996.

Gloersen, P, and A. Mernicky, Oscillatory behavior in Antarctic sea ice concentrations, in *AGU Antarctic Research Series: Antarctic Sea Ice: Physical Processes, Interactions and Variability* **74**, M.O. Jeffries, ed., 161-171, 1998.

Kuo, C., C. R. Lindberg, and D. J. Thomson, Coherence established between atmospheric carbon dioxide and global temperature, *Nature* **343**, 709-714, 1990.

Lindberg, C. R., Multiple taper spectral analysis of terrestrial free oscillations, Ph.D. thesis, Univ. of Calif., San Diego, 1986.

Lindberg, C. R., and J. Park, Multiple-taper spectral analysis of terrestrial free oscillations, II, *Geophys. J. R. Astron. Soc.* **91**, 795-836, 1987.

Maykut, G. A., Energy exchange over young sea ice in the central Arctic, *J. Geophys. Res.* **83**, 3646-3658, 1978.

Parkinson, C. L., Spatial patterns in the length of the sea ice season in the Southern Ocean, 1979-1986, *J. Geophys. Res.* **99**, 16,327-16,339, 1994.

Parkinson, C. L., D. J. Cavalieri, P. Gloersen, H. J. Zwally, and J. C. Comiso, Variability of the Arctic sea ice cover 1978-1996, *this issue.*

Parks, T. W., and C. S. Burrus, Chapter 7 in *Digital Filter Design*, John Wiley and Sons, New York, 1987.

Simmonds, I., and W. F. Budd, A simple parameterization of ice leads in a general circulation model, and the sensitivity of climate to change in Antarctic ice concentration, *Ann. Glaciol.* **14**, 266-269, 1990.

Zwally, H. J., J. C. Comiso, C. L. Parkinson, D. J. Cavalieri, and P. Gloersen, Variabiity of Antarctic sea ice from satellite observations, *in preparation.*

Zwally, H. J., J. C. Comiso, and A. L. Gordon, Antarctic offshore open water within the pack and oceanographic effects, in *Oceanology of the Antarctic Continental Shelf*, S. S. Jacobs, ed., Antarctic Research Series vol. 43, American Geophysical Union, Washington, D. C., pp. 203-226, 1985.

List of Figures

Figure 1. Plot of the time-series of the sum of the Arctic and Antarctic ice extents, areas, and open water areas within the pack.

Figure 2. Band-limited regression trends in the sums of Arctic and Antarctic ice extents, areas, and open water areas within the pack. The trends are superimposed on data that have been annually smoothed with a Butterworth filter, for ease of comparison. The trends were obtained from the data prior to smoothing.

Plate 1. Maps of (a) and (b) 18-year means of the Arctic and Antarctic sea ice concentrations, and (c) and (d) their seasonal cycle amplitudes, taken as the rms of the amplitudes of the 5 harmonic components of the annual cycle (see text).

Plate 2. Maps of the 18-year trends in the Arctic and Antarctic sea ice concentrations, and their confidence levels. (a) Arctic trends. (b) Antarctic trends. (c) Arctic confidence levels. (d) Antarctic confidence levels.

Plate 3. Maps of the amplitudes and phases of the modeled annual cycles in the Arctic and Antarctic sea ice concentrations. (a) Arctic amplitude. (b) Antarctic amplitude. (c) Arctic phase. (d) Antarctic phase.

Plate 4. Maps of the amplitudes of the modeled semi-and 1/3-annual cycles in the Arctic and Antarctic sea ice concentrations. (a) Arctic semi-annual amplitude. (b) Antarctic semi-annual amplitude. (c) Arctic 1/3-annual amplitude. (d) Antarctic 1/3-annual amplitude.

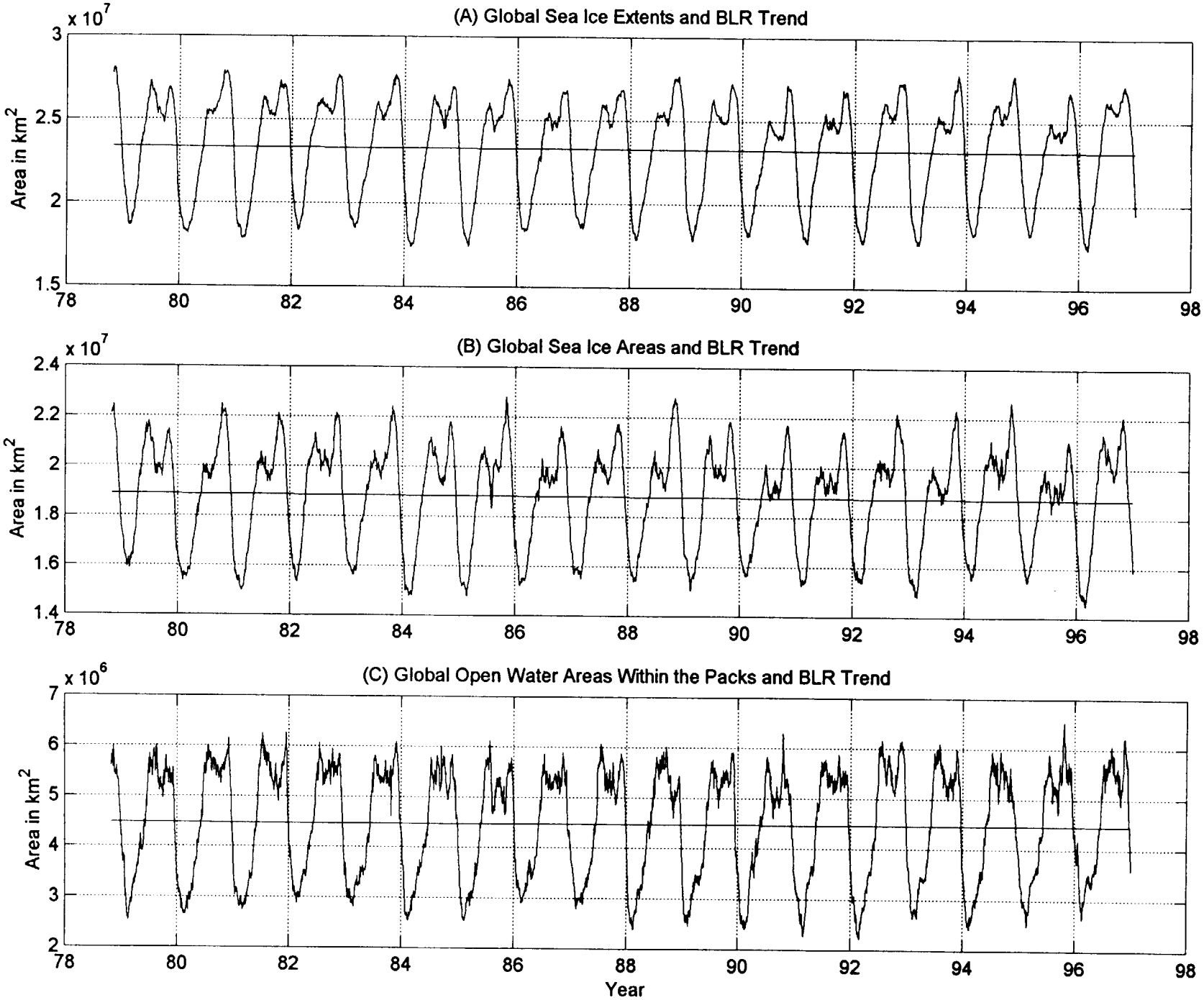
(A) Global Sea Ice Extents and BLR Trend
x 10^7
Area in km^2
3
2.5
2
1.5
78
80
82
84
86
88
90
92
94
96
98
(B) Global Sea Ice Areas and BLR Trend
x 10^7
Area in km^2
2.4
2.2
2
1.8
1.6
1.4
(C) Global Open Water Areas Within the Packs and BLR Trend
x 10^6
Area in km^2
7
6
5
4
3
2
Year

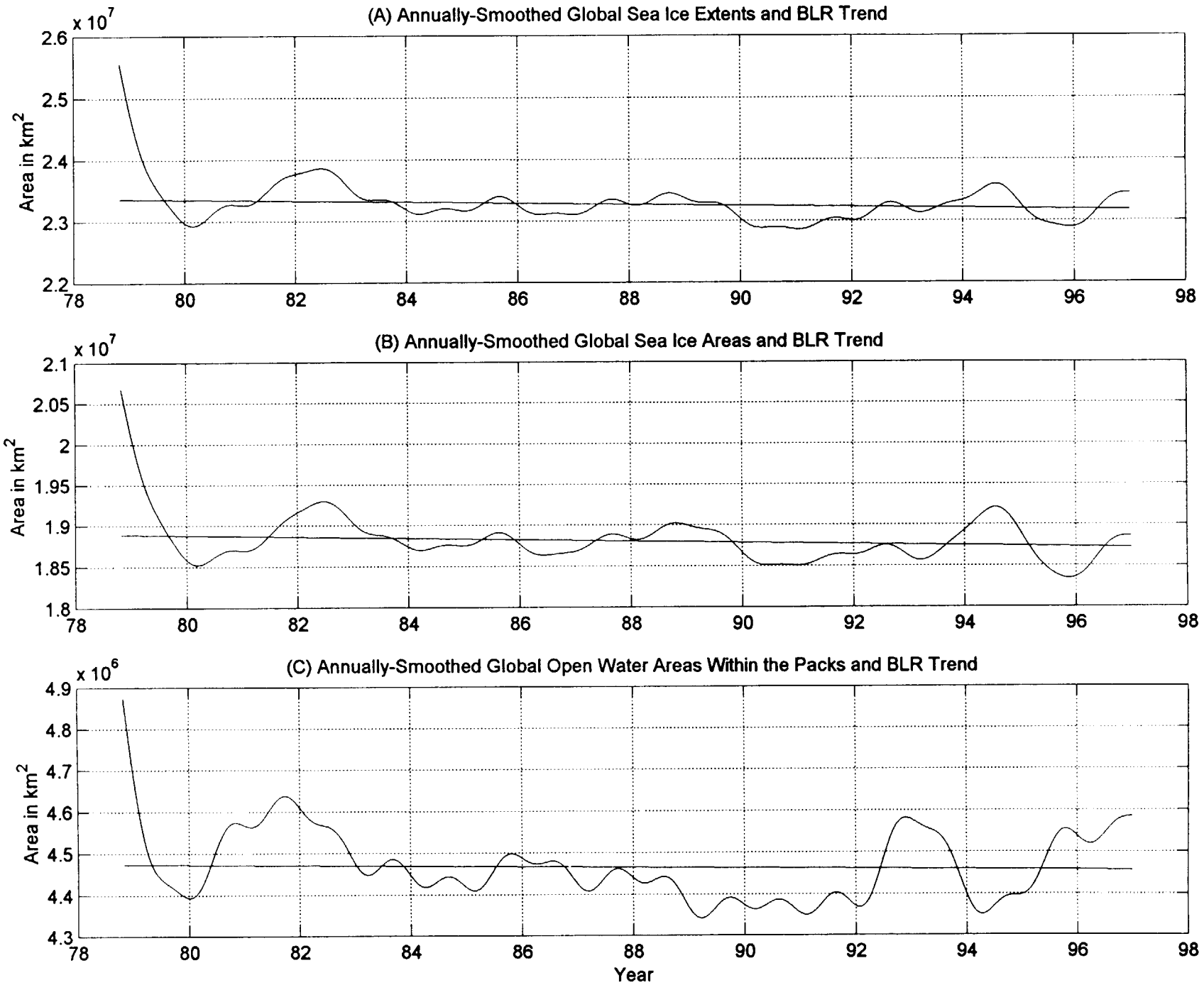
(A) Annually-Smoothed Global Sea Ice Extents and BLR Trend
x 10^7
Area in km^2
2.6
2.5
2.4
2.3
2.2
78
80
82
84
86
88
90
92
94
96
98
(B) Annually-Smoothed Global Sea Ice Areas and BLR Trend
x 10^7
Area in km^2
2.1
2.05
2
1.95
1.9
1.85
1.8
(C) Annually-Smoothed Global Open Water Areas Within the Packs and BLR Trend
x 10^6
Area in km^2
4.9
4.8
4.7
4.6
4.5
4.4
4.3
Year

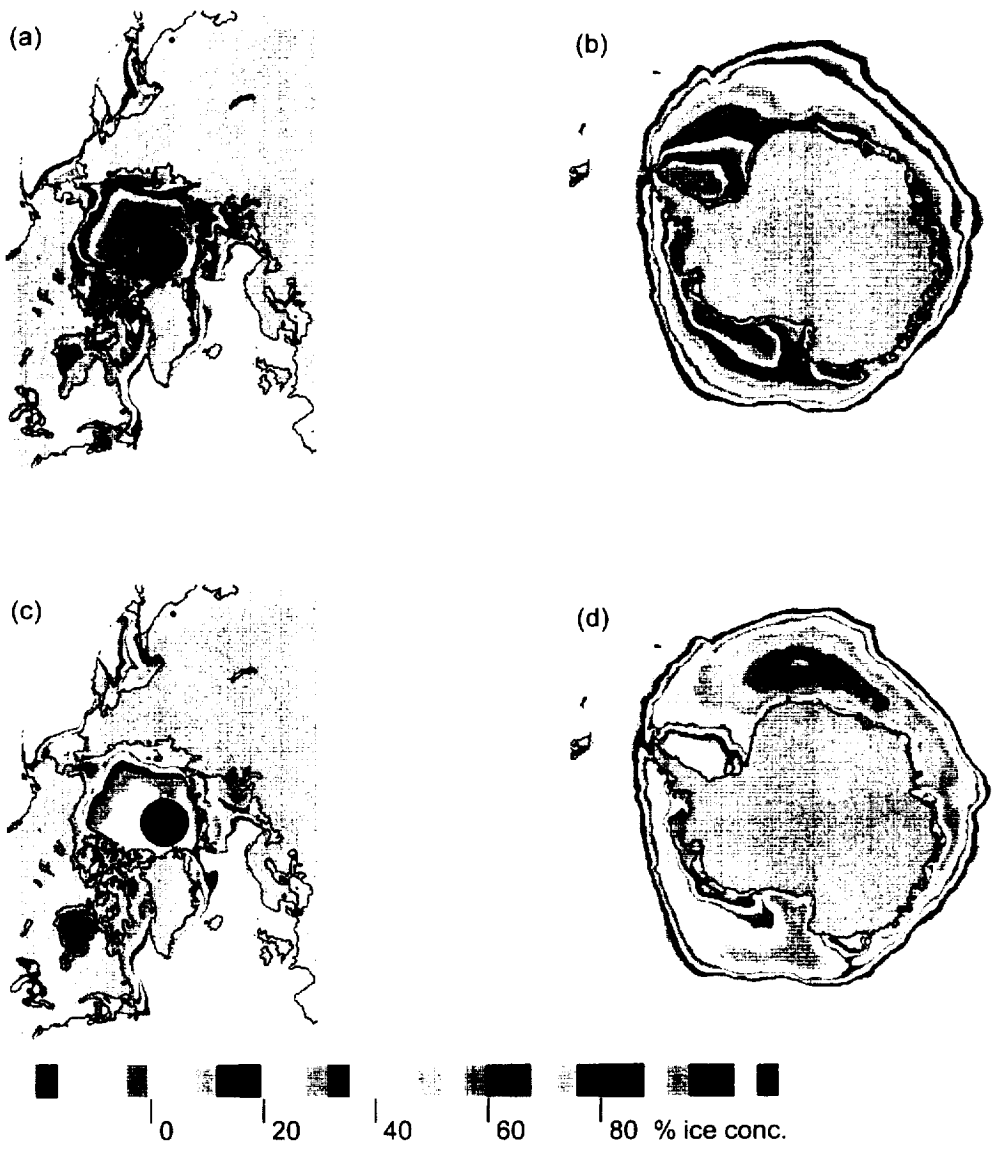
(a)
(b)
(c)
(d)
0
20
40
60
80
% ice conc.

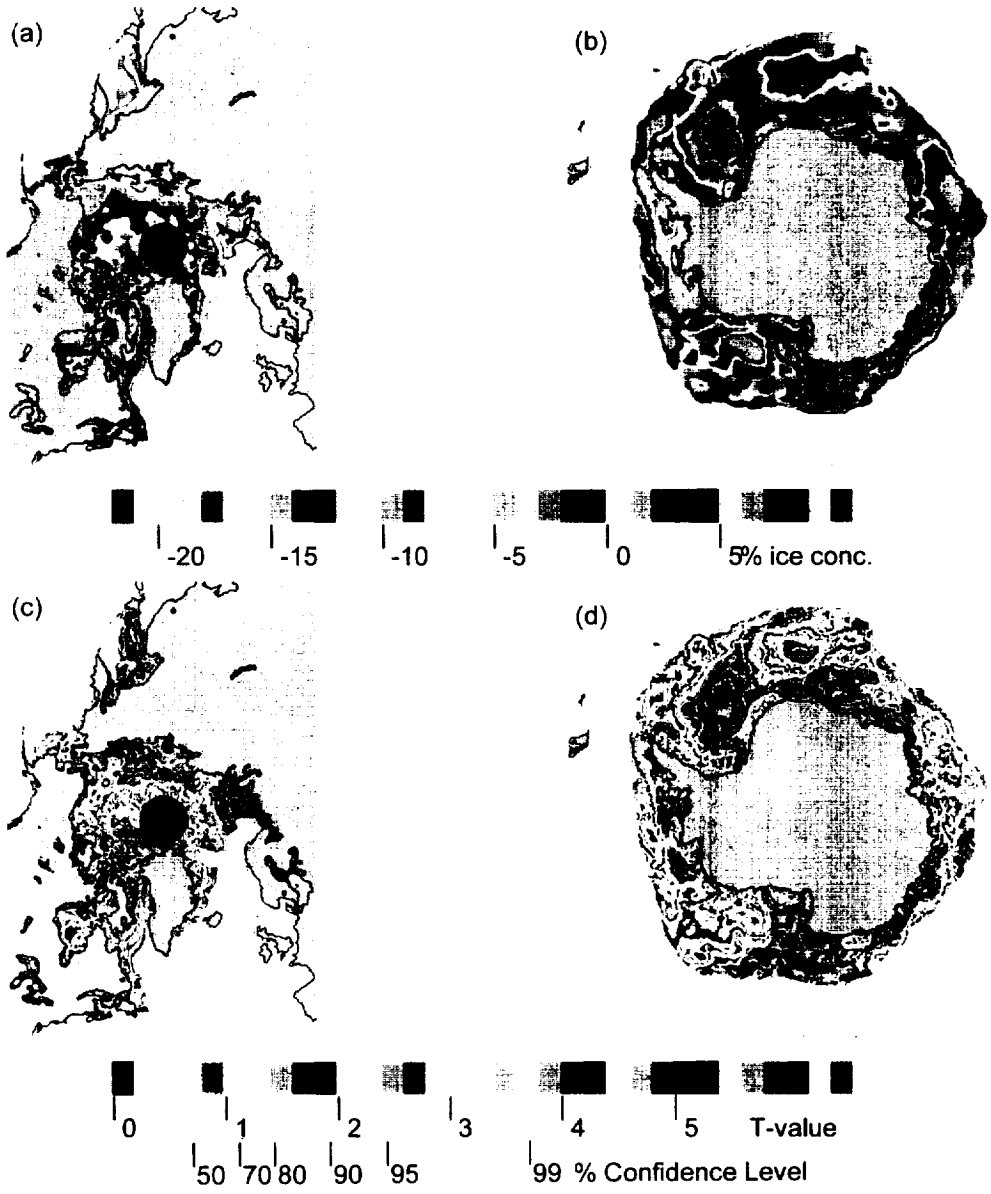
(a)
(b)
-20
-15
-10
-5
0
5% ice conc.
(c)
(d)
0
1
2
3
4
5
T-value
50
70
80
90
95
99
% Confidence Level

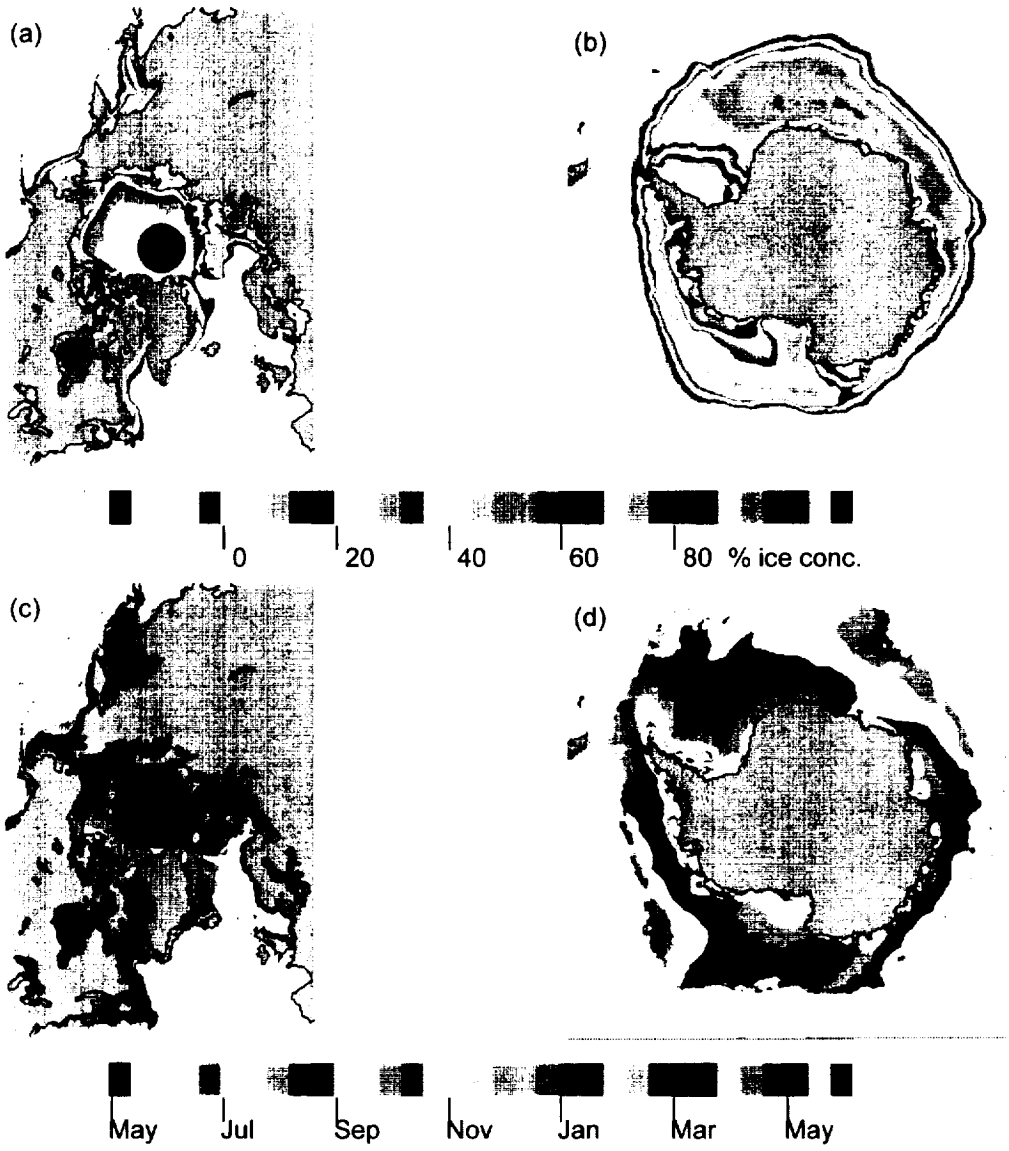
(a)
(b)
0
20
40
60
80
% ice conc.
(c)
(d)
May
Jul
Sep
Nov
Jan
Mar
May